Applied Physics Letters

Phonon-induced plasmon-exciton coupling changes probed via oscillation-associated spectra

Cite as: Appl. Phys. Lett. **115**, 111903 (2019); https://doi.org/10.1063/1.5116836
Submitted: 30 June 2019 . Accepted: 02 August 2019 . Published Online: 13 September 2019

Matthew S. Kirschner, Yeonjun Jeong, Austin P. Spencer, Nicolas E. Watkins, Xiao-Min Lin, George C. Schatz, Lin X. Chen, and Richard D. Schaller

Applied Physics Letters ARTICLE scitation.org/journal/apl

Phonon-induced plasmon-exciton coupling changes probed via oscillation-associated spectra

Cite as: Appl. Phys. Lett. **115**, 111903 (2019); doi: 10.1063/1.5116836
Submitted: 30 June 2019 · Accepted: 2 August 2019 ·
Published Online: 13 September 2019

View Online Export Citation CrossMark

Matthew S. Kirschner,[1] Yeonjun Jeong,[1] Austin P. Spencer,[1] Nicolas E. Watkins,[1] Xiao-Min Lin,[2] George C. Schatz,[1] Lin X. Chen,[1,3] and Richard D. Schaller[1,2,a)]

AFFILIATIONS

[1]Department of Chemistry, Northwestern University, 2145 Sheridan Rd., Evanston, Illinois 60208, USA
[2]Center for Nanoscale Materials, Argonne National Laboratory, 9700 Cass Ave., Argonne, Illinois 60439, USA
[3]Chemical Sciences and Engineering Division, Argonne National Laboratory, 9700 Cass Ave., Argonne, Illinois 60439, USA

[a)]**Author to whom correspondence should be addressed:** schaller@anl.gov and schaller@northwestern.edu

ABSTRACT

Coherent vibrations detected in optical experiments can offer insights into material properties and electronic interactions, but also yield complex time-dependent optical signatures, especially in hybridized systems. Here, we adapt techniques from studies on vibrational wave packets in molecules to analyze the optical signatures of coherent acoustic phonons in nanoparticles. This strategy enables us to better understand the implications of energetic changes induced by coherent phonons. We then apply this approach to systems that target coherent acoustic phonons as a route to modulate plasmon-exciton coupling and compare the results to theoretical calculations. Taken together, the described approach provides an intuitive, simple means of analyzing future systems and facilitates attempts to utilize, rather than simply observe, nanomaterial phonon modes.

https://doi.org/10.1063/1.5116836

Following impulsive electronic excitation of a nanoparticle, a portion of that energy can be converted rapidly to lattice motion via the generation of phonons. When phonons of a specific frequency are launched significantly faster than their period, coherent (in phase) oscillations in particle geometry can occur which often modulate the optical properties.[1–18] In particular, low-energy acoustic phonons in finite-size nanoparticles, which typically present challenges for conventional Raman spectroscopy to detect, can be characterized in the time domain enabling unique insights into the material properties.[11,12] Additionally, these phonon modes can be affected by small mass changes and used to perform mass sensing with up to yoctogram resolution.[13,14] Recently, it has been observed that coherent phonons can modulate electronic coupling between systems.[3,19,20] Particularly of note are hybrid materials that exhibit plasmon-exciton coupling[21–23] which can be modified by phonons to yield oscillatory plasmonic-excitonic nanomaterials (OPENs).[3] As the field advances, it should be possible to use the induced changes in electronic properties in other contexts such as manipulating electron or energy transfer to or from nanomaterials.

Coherent acoustic phonons are typically characterized by analyzing optical transient absorption (TA) spectra to determine the frequencies of the populated phonon modes. While this approach reveals the frequency of the mechanical changes, it does little to clarify the electronic implications of this phenomenon. Occasionally, a more sophisticated transient spectral analysis is used wherein at every time point, the TA spectrum is fit to the difference of the ground state spectrum and a spectrally shifted excited-state spectrum which can be used to quantify particle expansion along a phonon mode.[15,16,18] However, this requires optical spectra with simple line shapes. Systems that take advantage of the induced electronic changes, such as OPENs, exhibit substantially more complex spectra with multiple peaks and highly asymmetric spectral features which confound this type of analysis.[3]

Here, we present a strategy for analyzing these more complex systems derived from previous methods used in analyzing vibrational wave packets in molecular systems.[24–31] This technique, which we refer to as oscillation associated spectrum (OAS) analysis, determines the phase and magnitude of the oscillatory dynamics at each individual wavelength to reveal information about the underlying phenomenon. We begin by describing the technique when analyzing gold bipyramid transient spectra—a prototypical ensemble that exhibits well-defined coherent acoustic phonons.[3,14,17,18] In addition to agreeing with conventional understanding of this system, OAS provides additional

insights from deconvoluting ensemble inhomogeneity. We proceed by demonstrating that this technique can extract effects of phonons in OPENs which agree well with theoretical calculations. We conclude by discussing other contexts where OAS is particularly advantageous. Moving forward, OAS can help facilitate design of systems that take advantage of phonon-induced electronic changes, e.g., phase-controlled applications.

Figure 1(a) shows a two dimensional TA map (TA signal vs wavelength and pump-probe delay) of a typical ensemble of gold bipyramids excited on their localized surface plasmon resonance (LSPR). Following the generation of phonons through electron-phonon coupling,[1,2] the spectra are dominated by two phenomena. First, heating of the lattice causes the plasmon resonance to broaden and redshift. Second, coherent acoustic phonons produce oscillations in LSPR energy. This bipyramidal phonon mode is known to involve elongation of the long axis and shortening of the short axis and vice versa. As the particles expand and contract, the LSPR red shifts and blue shifts, respectively, resulting in the observed periodic behavior. To characterize the effects dominated by coherent acoustic phonons, we begin by subtracting away the nonoscillatory components of the data. To this end, we made use of the matrix pencil method to model exponential decays and damped oscillations simultaneously as a sum of complex exponentials at each wavelength, using information theoretic criteria to determine the optimal number of exponential functions.[32] By modeling both oscillatory and nonoscillatory components simultaneously, these signals can be more cleanly separated. The resulting 2D TA map isolating the oscillatory component is displayed in Fig. 1(b). Notably, the magnitude of the oscillations is distinct from the amplitude of the overall transient signal. Furthermore, there is a nodal line near the static extinction maximum (denoted by a dashed gray line) representing a change of phase in the oscillations. This phase reversing behavior is also observed for acoustic phonons in other nanomaterials including nanospheres and nanorods.[4,15]

To gain a more quantitative understanding, we performed Fourier transformations at every wavelength as is commonly done in analyzing vibrational wave packets in molecular systems.[24–30] Averaged together, the maximum Fourier transform magnitude here occurred at a frequency of 28.7 GHz (period of 34.8 ps, FWHM of 9.0 GHz). Figure 2(a) demonstrates how the phases of the oscillations vary with the wavelength at this frequency. To better illustrate trends, these phases are reported relative to a frequency-dependent reference phase to yield

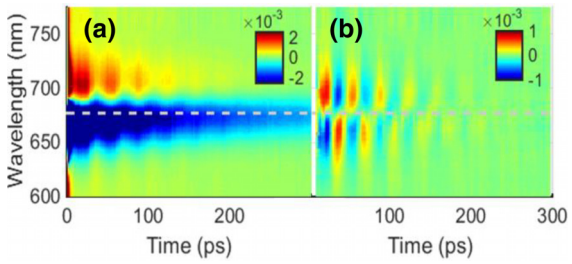

FIG. 1. (a) A 2D TA map of a photoexcited bipyramid ensemble with an LSPR of 677 nm indicated with a dashed gray line. (b) A TA map following subtraction of nonoscillatory dynamics from panel A with the static LSPR maximum indicated by a dashed gray line.

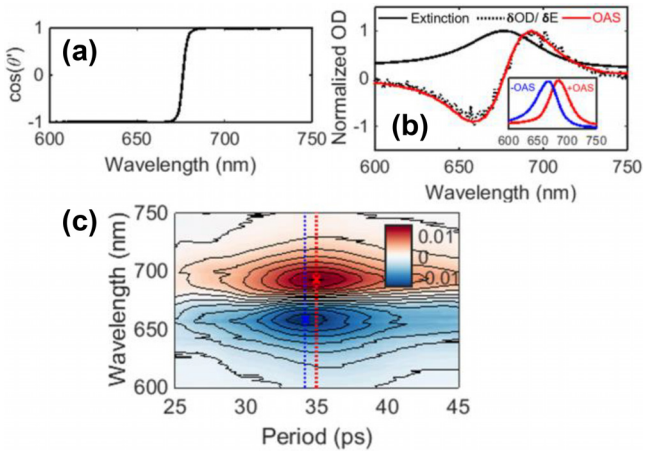

FIG. 2. (a) Relative phase $\cos(\theta')$ of bipyramid oscillations at a period of 34.8 ps. (b) Normalized extinction spectrum of the bipyramid ensemble (solid black), the derivative of that spectrum with respect to photon energy (dashed black), and the OAS (solid red). Inset: the extinction spectrum plus (red) and minus (blue) the OAS. (c) 2D map of the OAS spectrum vs oscillation period with contour lines.

$$\theta'(\lambda,f) = \theta(\lambda,f) - \theta_0(f),$$

where λ is the wavelength, f is the oscillation frequency, and θ', θ, and θ_0 are the reported, observed, and reference phases, respectively. We here use the convention that $\theta' = 0$ corresponds to the particle being expanded along its long axis at time zero, consistent with initial particle expansion following photoexcitation. Theoretical calculations show the expansion results in the LSPR red-shifting which increases extinction at photon energies lower than the LSPR. Thus, we define θ_0 as

$$\theta_0(f) = \frac{\int_{\lambda_{max}}^{\lambda_{end}} \theta(\lambda,f)\mathrm{d}\lambda}{\lambda_{end} - \lambda_{max}}.$$

In this case, $\lambda_{max} = 690$ nm and $\lambda_{end} = 714$ nm. We specifically display $\cos(\theta')$ as it outputs a value of 1 if a feature is perfectly in phase with initial particle expansion and –1 if it is out of phase. This change in the oscillation phase is sharp and well-defined as a result of the behavior originating from a single phenomenon: coherent phonons simultaneously cause some regions to increase in extinction and other regions to decrease. This simplicity in phase behavior enables phonon-induced changes in extinction to be spectrally described by multiplying the relative phase with the Fourier transform magnitude. We refer to the resulting product as the afore-mentioned oscillation associated spectra (OAS) because these describe the spectral changes induced by the vibrations in analogy to the decay associated spectra that describe how electronic excited states change the optical properties of a molecular system.[33–35] This method for calculating the OAS is equivalent to taking the real-part of the Fourier-transformed signal where the phase origin has been set to θ_0. Mathematically,

$$\mathrm{OAS}(\lambda,f) = \mathrm{Re}\left\{\mathcal{F}_t[\Delta A(\lambda,t)] \times e^{-i\theta_0(f)}\right\},$$

where $\Delta A(\lambda,t)$ is the observed change in the absorbance of the sample at wavelength λ after time t following photoexcitation of the LSPR, $\mathcal{F}_t[\Delta A(\lambda,t)]$ is the Fourier transform with respect to t of $\Delta A(\lambda,t)$ to

yield $\Delta A(\lambda, f)$ and Re is the real-part function. The inclusion of phase information in analyzing oscillatory dynamics, as in the OAS approach, is not frequently applied in molecular systems as their phase behavior is more complex; OAS best describes phase shifts that are exactly π. Rather, OAS uses the same underlying logic as the damped oscillation associated spectra, although the simpler phase behavior of acoustic phonons in a nanomaterial makes the implementation and interpretation much simpler.[31]

The OAS of this sample at a frequency of 28.7 GHz (34.8 ps period) is shown in Fig. 2(b). As acoustic phonons cause a plasmonic particle to expand and contract, often it is assumed that the plasmon resonance red shifts and blue shifts while retaining the same general structure. With a constant peak structure, the extinction at any given wavelength will be determined by its proximity to the extinction maximum. Therefore, as coherent acoustic phonons cause the LSPR to shift, the extinction at any given wavelength will change based on its updated proximity to the extinction maximum. The magnitude of this change will be proportional to how extinction changes with relative proximity to the LSPR, which are equivalent to the changes in energy. In terms of observables, the amplitude of extinction changes resulting from oscillations in LSPR energy should be proportional to the derivative of the static extinction spectrum with respect to energy. This trend is evident in Fig. 2(b), where the OAS matches up well with the derivative of the static extinction with respect to energy. In the inset, we demonstrate how the extinction spectrum would change if it was solely affected by coherent acoustic phonons by adding (red) or subtracting (blue) the OAS from the static extinction spectrum. Unsurprisingly, the resulting spectra simply suggest the LSPR is red shifting and blue shifting. Peak broadening or red shifting from incoherent heating both contradict the assumptions in our discussion and could create differences between the OAS and the derivative of the extinction spectrum, although these effects are generally quite small[18] justifying our neglect of them. In Fig. S1, we demonstrate that the similarity between OAS and the differentiated extinction spectrum is consistent across the bipyramids we have examined. It is worth mentioning that Hartland had previously considered the Fourier transform magnitude of phonons in gold nanospheres as a function of wavelength and found a maximum magnitude at a wavelength red of the LSPR.[15] That observation was likely the result of the same trend we describe above as it was caused by an analogous phenomenon.

In addition to confirming these conventional assumptions about acoustic phonons, OAS provides a method of deconstructing inhomogeneity in the ensemble. Phonon frequencies are dependent on the particle geometry so particles with different sizes oscillate at slightly different frequencies. These differences cause inhomogeneous dephasing which dominate dynamics in most nanoparticle ensembles[1,2] and consequently highly monodisperse nanoparticles—including gold bipyramids—are the focus of many coherent acoustic phonon studies.[3,5,14,16–18] However, in the analysis of such systems, inhomogeneity is considered only in the context of dephasing rates without considering that different particles present different extinction spectra and oscillation frequencies. There have also been some single particle measurements on coherent acoustic phonons which are able to circumvent issues of inhomogeneity,[6–8,11] but phonon-driven application will require ensembles of nanomaterials. OAS resolves the issue of inhomogeneity by considering the oscillation frequency at every wavelength independently. Figure 2(c) which shows a 2D map of the OAS. These are the same positive and negative features as shown in Fig. 2(b)—which is essentially a line cut of this 2D map—but these two features have distinct spectral-phonon frequency behaviors. Notably, the longer wavelength features tend to exhibit larger average periods. The oscillation period is known to increase with the particle length and the LSPR wavelength increases with the aspect ratio (length over width). It therefore makes sense that longer bipyramids also have higher aspect ratios resulting in the observed trend.

This methodology can also be applied to systems that exhibit more complex transient optical signals such as OPENs. Figure 3(a) shows a 2D TA map of the bipyramids from Figs. 1 and 2 decorated with a thiacarbocyanine dye, 2,2′-dimethyl-8-phenyl-5,6,5′,6′-dibenzothiacarbocyanine chloride (TCC). Following functionalization, the bipyramids electronically couple with TCC, resulting in two hybridized resonances with a Rabi splitting of 120 meV.[3] The TA spectra of the resulting ensemble system exhibits oscillatory behavior across its entire extinction spectrum from the coherent acoustic phonons of the bipyramids. These oscillations are quite challenging to interpret; in addition to having nonoscillatory dynamics to contend with, the extinction has a complex line shape making it difficult to extract the phonon induced spectral changes. As a result, previous analysis[3] was simplistic although, some insight into the underlying phenomena was gained. First, based on qualitative observations, it was argued that peak positions shift in phase with each other. Specifically, both hybridized resonances increase in energy and then, together, decrease in energy. This trend is consistent with predictions from a simple coupled oscillator model[36] as is used to describe plasmon-exciton coupling.[37,38] Second, based on Finite-Difference Time-Domain (FDTD) calculations, it was argued that the peak intensities change out of phase with one another; while one increases, the other decreases. This was interpreted through the lens of most of the oscillator strength of the resonances coming from the bipyramids rather than the TCC molecules. As acoustic phonons cause the LSPR to redshift; the redder peak has a

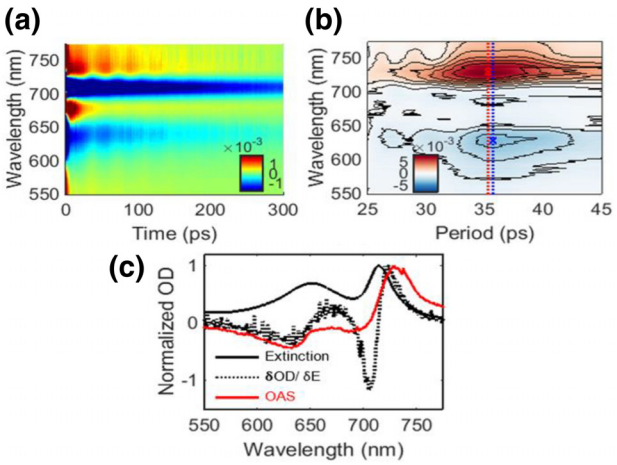

FIG. 3. (a) A 2D TA map of a gold bipyramid ensemble functionalized with TCC to create an OPEN. (b) A 2D OAS map of the OPEN ensemble. (c) Normalized extinction spectrum of the OPEN ensemble (solid black), the derivative of that spectrum with respect to photon energy (dashed black), and the OAS (solid red).

relatively more bipyramid character and thus a higher extinction cross section. While the experimental results were consistent with these scientific explanations, the spectra were sufficiently complex so that the experimental results merely supported models rather than providing independent information on which models could be built.

Fortunately, OAS is agnostic to the line shape and can overcome this complexity. It is briefly worth noting that OPENs exhibit the same simple phase behavior as bipyramids (Fig. S2) as they have the same underlying phenomenon of coherent acoustic phonons, validating the usage of the OAS. The 2D map of the OAS is displayed in Fig. 3(b). There is an overall shift in frequency with the maximum Fourier transform magnitude at a frequency of 28.2 GHz/35.4 ps period (FWHM 8.2 GHz). This change to lower frequency is likely due to the mass added by the dye, further conveying the prospective utility of gold bipyramids in mass sensing applications.[14] Relatedly, the period of the oscillations in the hybridized systems seems to be longer at bluer wavelengths. This may be due to the fact that the higher-energy peak is more TCC-like in character, as it should be more intense for particles that have more TCC attached to the bipyramid, which would increase the oscillation period.

The OAS at the maximum Fourier transform magnitude is shown in Fig. 3(c) along with the static extinction spectrum and the derivative of the static extinction spectrum. In contrast to bare gold bipyramids, the OAS of an OPEN sample resembles—but does not match—the derivative of its extinction spectrum. This difference suggests that the behavior is more complex than a simple shift in the peak position. However, the shape of the OAS could be explained by changes in the relative amplitude of the two peaks. The spectral region between the two peaks would have competing factors from changes in the peak amplitude and peak position changes which could result in the observed reduced oscillation strength and phase behavior. This trend is indeed observed in Fig. S3(a) where the OAS is added or subtracted from the static extinction spectrum. It becomes clear that particle expansion causes both resonances to red shift with the redder peak increasing in intensity and the bluer peak decreasing in intensity. Conversely, particle contraction causes the peaks to blue shift with the bluer peak increasing in intensity while the redder peak decreases in intensity. It is worth comparing these results to theoretical (electrodynamics combined with continuum mechanics) calculations that were used to generate the original scientific model.[3] To accomplish this task, we performed a series of FDTD calculations. Bipyramids were coated with a TCC layer and then were expanded or contracted 1% along their lowest order acoustic phonon mode. The extinction spectra of these modified particles, along with those of the particle in its original geometry are also shown in Fig. S3(b). These calculations and the experimental data analyzed with OAS are strikingly similar, demonstrating experimental evidence of the proposed model.

In addition to improving our specific understanding of this nanoparticle system, it is worth considering the utility of OAS in several contexts. A major strength of OAS is its simplicity, which makes it scalable for especially complex or crowded spectra. For example, if there were multiple phonons of different frequencies affecting the dynamics at similar wavelengths, their separation in frequency space would make it trivial for OAS to separate their effects. Further, due to its lack of assumptions about line shape, it could also be used to evaluate changes in the peak width or even the emergence of additional resonances. While this work uses OAS in the context of broadband probes, this strategy could be employed with a more limited set of probe wavelengths. For example, examining the oscillation phase and amplitude at the extinction maximum relative to the derivative maximum of the extinction spectrum (two separate wavelengths) could help identify whether a resonance is changing in energy, as observed here, or changing in amplitude as has been observed in TiO_2.[10] Fewer probe wavelengths monitored impede deconvolution of multifarious spectra, and many more than two wavelengths, around ten, would be needed to evaluate the behavior of OPENs. In other words, the number and selection of the wavelengths required depends on the complexity of the spectral changes induced by the oscillatory phenomenon.

In conclusion, we have described OAS and applied it to analyze coherent acoustic phonons in nanomaterials. We validated the assumption that phonons cause shifts in LSPR energy—with minimal changes in the line shape—while refining insights into sample inhomogeneity. OAS also experimentally validated previously suggested models of phonon-induced changes in plasmon-exciton coupling in OPENs. This general strategy could be used to analyze oscillatory effects, such as from phonons or other periodic signals, on arbitrarily complex systems and aid in the design of applications that use the coherent phonons of nanomaterials.

See the supplementary material for OAS analysis of another gold bipyramid ensemble, relative phase analysis, theoretical calculation results pertaining to particle expansion, and additional experimental methods.

We acknowledge support from the Ultrafast Initiative of the U.S. Department of Energy, Office of Science, Office of Basic Energy Sciences, through the Argonne National Laboratory under Contract No. DE-AC02-06CH11357. Use of the Center for Nanoscale Materials, an Office of Science user facility, was supported by the U.S. Department of Energy, Office of Science, Office of Basic Energy Sciences, under Contract No. DE-AC02-06CH11357. We acknowledge support from the National Science Foundation Graduate Research Fellowship Program under Grant No. DGE-1324585 (N.E.W.).

REFERENCES

[1]G. V. Hartland, Chem. Rev. **111**, 3858 (2011).
[2]T. A. Major, S. S. Lo, K. Yu, and G. V. Hartland, J. Phys. Chem. Lett. **5**, 866 (2014).
[3]M. S. Kirschner, W. Ding, Y. Li, C. T. Chapman, A. Lei, X. Lin, L. X. Chen, G. C. Schatz, and R. D. Schaller, Nano Lett. **18**, 442 (2018).
[4]M. Hu, X. Wang, G. V. Hartland, P. Mulvaney, J. P. Juste, and J. E. Sader, J. Am. Chem. Soc. **125**, 14925 (2003).
[5]K. O'Brien, N. D. Lanzillotti-Kimura, J. Rho, H. Suchowski, X. Yin, and X. Zhang, Nat. Commun. **5**, 4042 (2014).
[6]P. V. Ruijgrok, P. Zijlstra, A. L. Tchebotareva, and M. Orrit, Nano Lett. **12**, 1063 (2012).
[7]K. Yu, P. Zijlstra, J. E. Sader, Q. Xu, and M. Orrit, Nano Lett. **13**, 2710 (2013).
[8]T. Devkota, D. Chakraborty, K. Yu, G. Beane, J. E. Sader, and G. V. Hartland, Phys. Chem. Chem. Phys. **20**, 17687 (2018).
[9]C. Yi, P. D. Dongare, M.-N. Su, W. Wang, D. Chakraborty, F. Wen, W.-S. Chang, J. E. Sader, P. Nordlander, N. J. Halas, and S. Link, Proc. Natl. Acad. Sci. **114**, 11621 (2017).
[10]E. Baldini, T. Palmieri, A. Dominguez, P. Ruello, A. Rubio, and M. Chergui, Nano Lett. **18**, 5007 (2018).
[11]P. Zijlstra, A. L. Tchebotareva, J. W. M. Chon, M. Gu, and M. Orrit, Nano Lett. **8**, 3493 (2008).

[12]P. Guo, R. D. Schaller, L. E. Ocola, J. B. Ketterson, and R. P. H. Chang, Nano Lett. **16**, 5639 (2016).
[13]J. Chaste, A. Eichler, J. Moser, G. Ceballos, R. Rurali, and A. Bachtold, Nat. Nanotechnol. **7**, 301 (2012).
[14]B. Dacosta Fernandes, M. Spuch-Calvar, H. Baida, M. Tréguer-Delapierre, J. Oberlé, P. Langot, and J. Burgin, ACS Nano **7**, 7630 (2013).
[15]G. V. Hartland, J. Chem. Phys. **116**, 8048 (2002).
[16]G. Soavi, I. Tempra, M. F. Pantano, A. Cattoni, S. Collin, P. Biagioni, N. M. Pugno, and G. Cerullo, ACS Nano **10**, 2251 (2016).
[17]M. Pelton, J. E. Sader, J. Burgin, M. Liu, P. Guyot-Sionnest, and D. Gosztola, Nat. Nanotechnol. **4**, 492 (2009).
[18]M. S. Kirschner, C. M. Lethiec, X. Lin, G. C. Schatz, L. X. Chen, and R. D. Schaller, ACS Photonics **3**, 758 (2016).
[19]P.-A. Mante, H.-Y. Chen, M.-H. Lin, Y.-C. Wen, S. Gwo, and C.-K. Sun, Appl. Phys. Lett. **101**, 101903 (2014).
[20]P. Ruello, A. Ayouch, G. Vaudel, T. Pezeril, N. Delorme, S. Sato, K. Kimura, and V. E. Gusev, Phys. Rev. B **92**, 174304 (2015).
[21]G. P. Wiederrecht, G. A. Wurtz, and J. Hranisavljevic, Nano Lett. **4**, 2121 (2004).
[22]N. T. Fofang, T. Park, O. Neumann, N. A. Mirin, P. Nordlander, and N. J. Halas, Nano Lett. **8**, 3481 (2008).
[23]N. T. Fofang, N. K. Grady, Z. Fan, A. O. Govorov, and N. J. Halas, Nano Lett. **11**, 1556 (2011).
[24]D. Polli, M. R. Antognazza, D. Brida, G. Lanzani, G. Cerullo, and S. De Silvestri, Chem. Phys. **350**, 45 (2008).
[25]M. Liebel and P. Kukura, J. Phys. Chem. Lett. **4**, 1358 (2013).
[26]P. C. Arpin, D. B. Turner, S. D. Mcclure, C. C. Jumper, T. Mirkovic, J. R. Challa, J. Lee, C. Y. Teng, B. R. Green, K. E. Wilk, P. M. G. Curmi, K. Hoef-emden, D. W. Mccamant, and G. D. Scholes, J. Phys. Chem. B **119**, 10025 (2015).
[27]S. D. Mcclure, D. B. Turner, P. C. Arpin, T. Mirkovic, and G. D. Scholes, J. Phys. Chem. B **118**, 1296 (2014).
[28]M. Liebel, C. Schnedermann, T. Wende, and P. Kukura, J. Phys. Chem. A **119**, 9506 (2015).
[29]S. Ruetzel, M. Diekmann, P. Nuernberger, C. Walter, B. Engels, and T. Brixner, J. Chem. Phys. **140**, 224310 (2014).
[30]P. Kim, M. S. Kelley, A. Chakraborty, N. L. Wong, R. P. Van Duyne, G. C. Schatz, F. N. Castellano, and L. X. Chen, J. Phys. Chem. C **122**, 14195 (2018).
[31]I. H. M. van Stokkum, C. C. Jumper, J. J. Snellenburg, G. D. Scholes, R. Van Grondelle, and P. Maly, J. Chem. Phys. **145**, 174201 (2016).
[32]Y. Lin, P. Hodgkinson, M. Ernst, and A. Pines, J. Magn. Reson. **128**, 30 (1997).
[33]R. Bonneau, J. Wirz, and A. D. Zuberbühler, Pure Appl. Chem. **69**, 979 (1997).
[34]A. K. Dioumaev, Biophys. Chem. **67**, 1 (1997).
[35]J. F. Nagle, Biophys. J. **59**, 476 (1991).
[36]S. Rudin and T. L. Reinecke, Phys. Rev. B **59**, 10227 (1999).
[37]P. Vasa, W. Wang, R. Pomraenke, M. Maiuri, C. Manzoni, G. Cerullo, and C. Lienau, Phys. Rev. Lett. **114**, 036802 (2015).
[38]A. E. Schlather, N. Large, A. S. Urban, P. Nordlander, and N. J. Halas, Nano Lett. **13**, 3281 (2013).